2022 International Conference on Rehabilitation Robotics (ICORR)
25-29 July, 2022, Rotterdam, The Netherlands

Development of inductive sensors for a robotic interface based on noninvasive tongue control*

Oguzhan Kirtas[1], Peter Veltink[2], Romulus Lontis[3], Mostafa Mohammadi[1], and Lotte N. S. Andreasen Struijk[1]

2022 International Conference on Rehabilitation Robotics (ICORR) | 978-1-6654-8829-7/22/$31.00 ©2022 IEEE | DOI: 10.1109/ICORR55369.2022.9896548

***Abstract*— Tongue based robotic interfaces have shown the potential to control assistive robotic devices developed for individuals with severe disabilities due to spinal cord injury. However, current tongue-robotic interfaces require invasive methods such as piercing to attach an activation unit (AU) to the tongue. A noninvasive tongue interface concept, which used a frame integrated AU instead of a tongue attached AU, was previously proposed. However, there is a need for the development of compact one-piece sensor printed circuit boards (PCBs) to enable activation of all inductive sensors. In this study, we developed and tested four designs of compact one-piece sensor PCBs incorporating inductive sensors for the design of a noninvasive tongue-robotic interface. We measured electrical parameters of the developed sensors to detect activation and compared them with a sensor of the current version of the inductive tongue-computer interface (ITCI) by moving AUs with different contact surfaces at the surface of the sensors. Results showed that, the newly developed inductive sensors had higher and wider activation than the sensor of ITCI and the AU with a flat contact surface had 3.5 - 4 times higher activation than the AU with a spherical contact surface. A higher sensor activation can result in a higher signal to noise ratio and thus a higher AU tracking resolution.**

I. Introduction

Disabilities due to spinal cord injury (SCI) are devastating for the affected people. The impairment of motor functions severely limits performing activities of daily living, independence, psychological wellbeing, and therefore quality of life [1], [2]. To restore motor functions and increase quality of life of affected individuals, robotic devices such as assistive manipulators [3] and exoskeletons [4] have been proposed.

Tongue functionality of individuals with SCI usually remains intact. Therefore, generation of highly reliable control input signals is possible with tongue based control systems due to the high flexibility of the tongue [5]. Additionally, tongue based interfaces can be preferable for the control of assistive robotic devices since they are not visible from outside and require low physical effort [6].

Recently, several tongue based robotic interfaces have been developed. The most advanced current tongue interfaces include the tongue-drive system (TDS) and the inductive tongue-computer interface (ITCI). The TDS provides 7 command signals [7] and has been used to control computers [8], a powered wheelchair [9], and a single degree of freedom (DOF) of a hand exoskeleton [10]. A higher number of command signals can be necessary for controlling an assistive robot, for example the JACO robotic arm requires 14 commands to fully control 7 DOF [5]. The ITCI provides 18 command signals [11] and it can control multiple grasps of a prosthetic hand [12], a 7 DOF robotic arm [5], and a 5 DOF upper limb exoskeleton [13]. Additionally, the ITCI has been commercialized as Itongue® for the control of personal computers and powered wheelchairs [14].

The ITCI comprises 18 inductive sensors made of 10-layer printed circuit board (PCB) coils which are divided into two sections constituting the keypad area and the mouse area (Fig. 1a). The inductance of a coil changes by moving an activation unit (AU) made of a ferromagnetic material close to the core of the coil due to the perturbations in the magnetic flux [15]. Thereby, an inductive sensor can function as a switch similar to a key of a remote control.

One challenge of the current tongue based robotic interfaces is the invasiveness. The TDS includes a magnetic tracer attached to the tongue by gluing or piercing [10]. Similarly, the ITCI requires gluing or piercing a metal AU to the tongue for the sensor activation. However, one third of potential users do not prefer the placement of a tongue piercing for a long-term use [16]. Additionally, the comfort level of the robotic interface devices is among the key factors determining the user acceptance [6]. Therefore, it could be beneficial to have a tongue-robotic interface which is smaller in size to reduce discomfort to the users and to allow for more space for tongue movements.

In [17], we developed a new noninvasive sensor activation method by mounting a frame with an integrated AU to the ITCI as a proof of concept for noninvasive tongue based robotic interfaces that does not require gluing or piercing an AU to the tongue. However, the current design of the ITCI with two angled positioned sensor PCBs only allows activating a portion of the sensors with a frame integrated AU. Thus, there is a need for the development of compact one-piece sensor PCBs with flat interaction surfaces to enable activation of all inductive sensors through a frame integrated AU. Additionally, previous studies have shown that inductive sensors with high sensitivity and interpolation of sensor signals to design virtual buttons and joysticks are desirable [15], [18]. Therefore, sensor PCBs should be optimized to increase the sensor activation and to reduce areas between

*This study is a part of the HyperHand project, supported by a grant from Offerfonden, Denmark.

[1]Oguzhan Kirtas, Mostafa Mohammadi, and Lotte N. S. Andreasen Struijk are with Neurorehabilitation Robotics and Engineering, Center for Rehabilitation Robotics, Department of Health Science and Technology, Aalborg University, Aalborg, Denmark (okr@hst.aau.dk, mostafa@hst.aau.dk, naja@hst.aau.dk)

[2]Peter Veltink is with Faculty of Electrical Engineering, Mathematics and Computer Science, University of Twente, Enschede, The Netherlands (p.h.veltink@utwente.nl)

[3]Romulus Lontis is with Neural Engineering and Neurophysiology, Center for Neuroplasticity and Pain, Department of Health Science and Technology, Aalborg University, Aalborg, Denmark (lontis@hst.aau.dk)

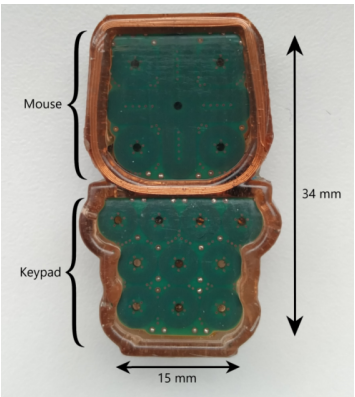

(a)

(b)

Fig. 1: (a) The keypad and mouse sensor PCBs of the ITCI and overall dimensions. (b) Activation units with flat contact surface (top) and spherical contact surface (bottom).

the sensor coils where no signal can be recorded.

In this paper, we developed and tested four different designs of compact one-piece sensor PCBs incorporating inductive sensor coils for the design of an interpolation based noninvasive tongue-robotic interface. We measured the electrical parameters of the developed sensor coils to detect activation and compared them with a coil of keypad area of the current version of the ITCI by moving AUs with different contact shapes at the surface of the coils.

II. Methods

A. Design of the inductive sensors

The keypad sensor PCB (Fig. 1a, bottom) of the current version of the ITCI had been designed in 10 layers and incorporated 10 round coils with 8.5 turns per layer. The mouse sensor PCB incorporated 4 round coils and 4 oval coils. The smallest width of the keypad sensor PCB was 15 mm, while total length of the sensor PCBs was 34 mm (Fig. 1a). The thickness of the ITCI sensor PCBs was 1 mm.

The requirements for the design of a new noninvasive tongue-robotic interface were incorporation of a compact one-piece sensor PCB, ensuring high sensor activation, and ensuring high performance interpolation of sensor signals. To satisfy these requirements,

- All of the one-piece flat PCB boards consisted of 15 coils in 3x5 configuration to reduce the overall size.
- The inductive sensors were designed in 12 layers PCB technology with increased number of coil turns per layer to increase the change in inductance by activation.
- The coils were made close to each other as much as possible since the AU position estimation error is higher in the spaces between the coils [18].

We selected two coil shapes: round (similar to the ITCI keypad coils) and rounded-square (to decrease the space between coils). Fig. 2 represents the longest inner length (D1) and outer length (D2) of the designed coils. Two of the designs incorporated 10 turns per layer, while the other two incorporated 9 turns. Therefore, D1/D2 lengths

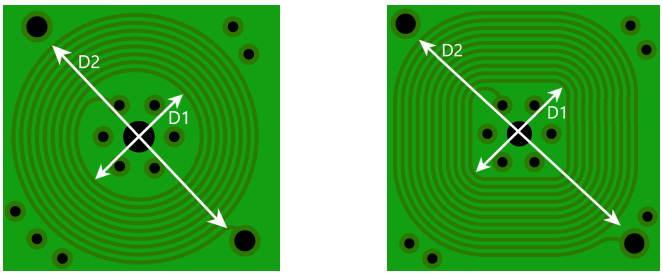

(a) Round coil. (b) Rounded-square coil.

Fig. 2: Highest inner lengths (D1) and outer lengths (D2) of the designed coils.

of the coils and board dimensions of the sensor PCBs were different. Table I summarizes the geometrical properties of the designed sensor PCBs and the keypad coils of the ITCI.

All of the coils were designed in 75 µm track and spacing width. Plated through-holes of 200 µm and pads of 400 µm were used for interlayer connection. Pads connecting the electronics were of 600 µm diameter with 400 µm through-holes. Non-plated through-holes of 600 µm for round and 500 µm for rounded-square were placed at the center of coils. Copper layers of 35 µm and 18 µm thicknesses were built on each side of cores, made from different thicknesses of standard woven epoxy glass materials (FR4). Six cores, with copper coating on both sides, were assembled in a sandwich structure (Fig. 3). The total thickness of the 12 layer PCB boards was 1.226 mm. Manufactured sensor PCBs can be seen in (Fig. 4) (Møn Print A/S, Denmark).

TABLE I: Geometrical properties of the designed sensor PCBs and the round keypad coils of the ITCI.

Coil Type	D1 / D2 (mm)	Layer Number	Coil Turn Number	Board Dimensions (mm) Width/Length/Thickness
Round, 15.9 mm width	2.4 / 4.95	12	120	15.9 / 26.475 / 1.226
Round, 15 mm width	2.4 / 4.65	12	108	15.0 / 25.975 / 1.226
Rounded-square, 15.9 mm width	2.5 / 5.35	12	120	15.9 / 25.350 / 1.226
Rounded-square, 15 mm width	2.5 / 5.05	12	108	15.0 / 23.850 / 1.226
Round keypad coils of the ITCI	2.4 / 4.50	10	85	15 / 34 / 1

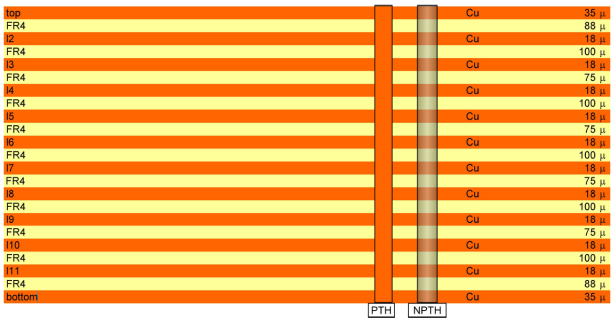

Fig. 3: Assembled sandwich structure of copper (Cu) and FR4 layers with different thicknesses. Total thickness of the sensor PCBs was 1.226 mm.

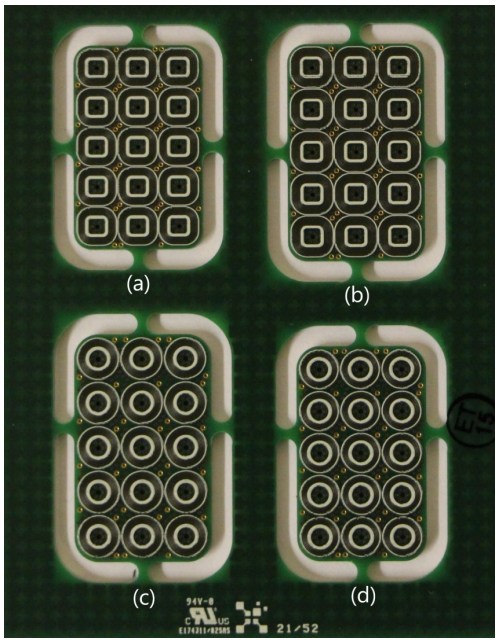

Fig. 4: Top view of the manufactured sensor PCBs. (a) 15 mm width PCB with rounded-square coils. (b) 15.9 mm width PCB with rounded-square coils. (c) 15.9 mm width PCB with round coils. (d) 15 mm width PCB with round coils.

B. Measurement of electrical parameters

We used a digital LCR meter (Keysight U1732C) with 10 kHz test frequency to measure electrical parameters of the coils of the developed PCBs and keypad coils of current version of the ITCI. First, we measured inductance and resistance values without activation for all coils of each type of PCBs to see the variation in the parameters might be caused due to the PCB manufacturing processes.

Then, we used two AUs made of biocompatible DYNA EFM alloy (61% palladium, 36.8% cobalt, 1% platinum and 2.2% other elements) with different contact surfaces for inductance measurements with activation. One of the AUs had a spherical shape with 4 mm diameter and other one had a flat circular contact surface with 4 mm diameter (Fig. 1b). We soldered the connections of the middle coil for each of the designed PCBs and the middle coil of the keypad sensor PCB of the ITCI for the inductance measurements.

We used a precision linear stage with two vertical axes and 0.01 mm precision to measure the inductance change of the coils by different AUs. We fixed the sensor PCBs, which were mounted on a bench vise, on the top of the linear stage. We fixed the AUs using another bench vise to ensure the contact between the AUs and sensor PCBs (Fig. 5).

We measured and recorded the inductance values while moving the sensor PCBs with 0.25 mm increments in the x and y axes for each step. Therefore, increments were 0.35 mm relative to the axis of center of AU movement (m-axis) defined in Fig. 6. The range for the measurements were -7.07 and +7.07 mm with respect to the center of measured coils (C_m) along the m-axis (-5 and +5 mm for x and y axes).

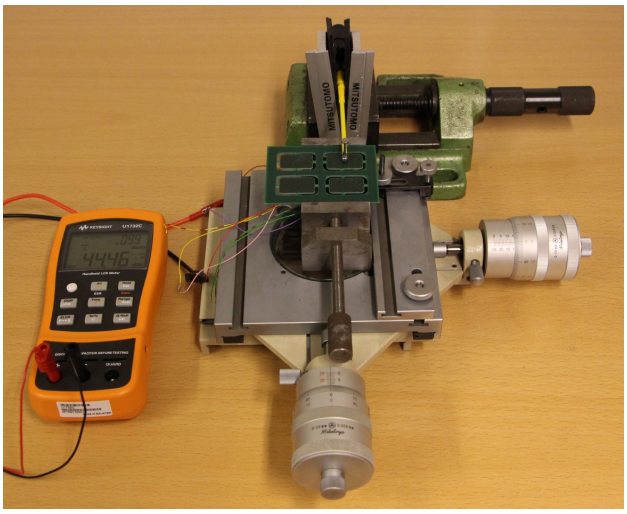

Fig. 5: An image of the setup for coil inductance measurements. Sensor PCBs were mounted on a linear stage and AUs were fixed using a bench vise to ensure contact.

Since we measured the inductance values of only one coil for each PCB, we superimposed the obtained results by the distance of the center of the diagonally neighbor coil (C_s) to the C_m to simulate the interpolation of sensor measurements for each sensor PCB. The distances from C_s to C_m can be seen in Table II.

TABLE II: The distances from the center of the measured coil (C_s) to the center of superimposed coil (C_m) for the developed sensor PCBs.

Coil Type	Distance (mm)
Round, 15.9 mm width	7.3
Round, 15 mm width	6.8
Rounded-square, 15.9 mm width	7.1
Rounded-square, 15 mm width	6.7
Keypad coils of the current TCI	7.0

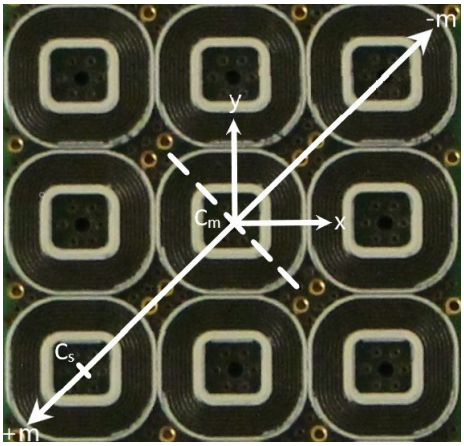

Fig. 6: Path for the inductance measurements along the m-axis. C_m and C_s are the center of measured coil and the center of superimposed coil, respectively.

III. Results

Table III shows the mean resistance (Ω) and inductance (μH) values of the 15 coils of the developed sensor PCBs and 10 coils of the keypad area of the ITCI without activation by an AU. Standard deviations are shown in parentheses. All of the developed sensor PCBs had higher mean resistance and inductance values than the keypad coils of the current version of the ITCI. Resistance and inductance values were higher in the PCB boards with 15.9 mm width than 15 mm width sensor PCBs. Rounded-square coils had slightly higher inductance and resistance than round coils. Highest mean inductance and resistance values were achieved by the 15.9 mm width sensor PCBs with rounded-square coils (42.3 μH and 29.3 Ω).

Table IV shows the induction values in μH of the middle coil of the developed sensor PCBs and the middle keypad coil of the current version of the ITCI when not activated and activated by an AU. L is the inductance without activation, L_s is the maximum inductance with activation by a spherical contact surface AU, and L_f is the maximum inductance with activation by a flat contact surface AU. Δ_{rel} (relative activation) shows the activation percentage by AUs with different contact surfaces relative to the inductance without activation. Relative activations were 6.6 - 7 % for the spherical contact surface AU and 24.3 - 26.4 % for the flat contact surface AU. Highest activation was achieved by the 15.9 mm width sensor PCBs with rounded-square coils (48.1 μH for the spherical AU and 56.2 μH for the flat AU).

Fig. 7 and Fig. 8 represent the change in inductance (μH) of the developed PCB coils and the keypad coils of the ITCI with respect to the movement of the AUs with spherical and flat contact surfaces. The curves in the left show the results for the measured middle coils of the sensor PCBs and the curves in the right show the superimposed results by the distance from C_s to C_m.

The flat contact surface AU resulted in 3.5 - 4 times higher change in induction and a wider range of activation than the spherical contact surface AU. All of the developed sensor PCBs had higher induction change and wider activation range than the keypad coil of the current version of the ITCI. Moreover, superimposition of the measured induction values resulted in closer curves for all of the sensor PCBs than the keypad area of the ITCI.

Sensor PCBs with 15.9 mm width had a higher change in induction than sensor PCBs with 15 mm width. Rounded-square coils led to slightly higher inductance change and slightly wider range of activation than round coils. Superimposed induction curves were closer to the curves of measured coils for the rounded-square coils than the round coils.

TABLE III: Mean resistance (Ω) and inductance (μH) values of the 15 coils of the developed sensor PCBs and 10 keypad coils of the ITCI. Standard deviations are shown in parentheses.

Coil Type	Mean Resistance (Ω)/ Standard Deviation (Ω)	Mean Inductance (μH) / Standard Deviation (μH)
Round, 15.9 mm width	27.8 / 0.6	38.8 / 0.4
Round, 15 mm width	23.2 / 0.5	30.2 / 0.3
Rounded-square, 15.9 mm width	29.3 / 0.9	42.3 / 0.4
Rounded-square, 15 mm width	26.0 / 0.8	33.5 / 0.4
Keypad coils of the current ITCI	18.1 / 0.1	23.3 / 0.5

IV. Discussion

Mean resistance and inductance values depend on the coil geometry and the total number of turns. All of the developed sensor coils had higher resistance and inductance than the keypad coils of the ITCI as a result of the increased coil turn number due to the increase in layer number. Sensor PCBs with 15.9 mm width had 26 - 28 % higher inductance values than 15 mm width PCBs as they incorporate coils with higher number of turns per layer. The reason for the slightly higher inductance and resistance values of the rounded-square coils is the slightly larger coil area due to the geometry of coils. Low standard deviations can be an indication of a good and consistent manufacturing process.

The relative activation percentages (Δ_{rel}) by the AU with flat contact surface were significantly higher for each type of PCB coils due to the larger contact surface. In addition to the higher change in induction, the range of the activation was higher for the AU with flat contact surface as it was in contact with the coils for a longer distance. Therefore, activation of the coils can be detected more easily with a flat contact surface AU. However, since the consistency of the results for flat the AU was affected by the imperfect contact surface, a better machining surface quality is required for the AUs with flat contact surface.

The relative activation percentage did not vary much with the type of the coil, therefore coils with higher inactive inductance had higher activation as well. A higher sensor activation means a higher signal to noise ratio and thereby a

TABLE IV: Induction values (μH) of the middle coils of the sensor PCBs when not activated and activated by an AU. L is the inductance when not activated, L_s is the maximum inductance when activated by a spherical contact surface AU, and L_f is the maximum inductance when activated by a flat contact surface AU. Δ_{rel} represents the activation percentage relative to the inductance without activation.

Coil Type	L (μH)	L_s(μH)/Δ_{rel}(%)	L_f(μH)/Δ_{rel}(%)
Round, 15.9 mm width	41.6	44.5 / 6.9	51.8 / 24.4
Round, 15 mm width	32.6	34.8 / 6.6	40.6 / 24.3
Rounded-square, 15.9 mm width	45.0	48.1 / 6.7	56.2 / 24.8
Rounded-square, 15 mm width	35.5	37.9 / 6.6	44.4 / 24.9
Keypad coil of the current ITCI	25.6	27.3 / 7.0	32.3 / 26.4

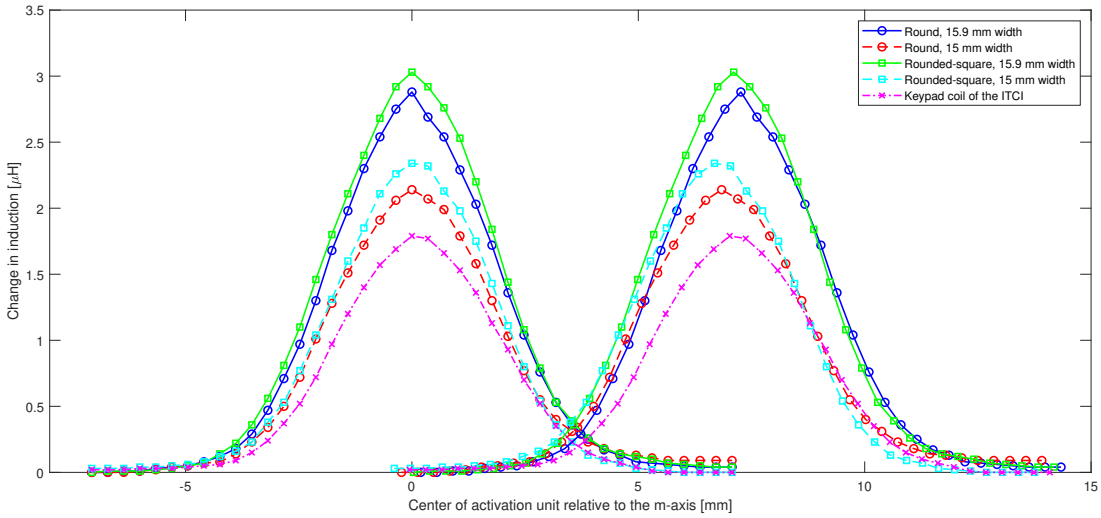

Fig. 7: The change in inductance of PCB coils with respect to the center of the AU with a spherical contact surface. The curves in the left show the results for the measured coils of the sensor PCBs and the curves in the right show the superimposed results by the distance from C_s to C_m.

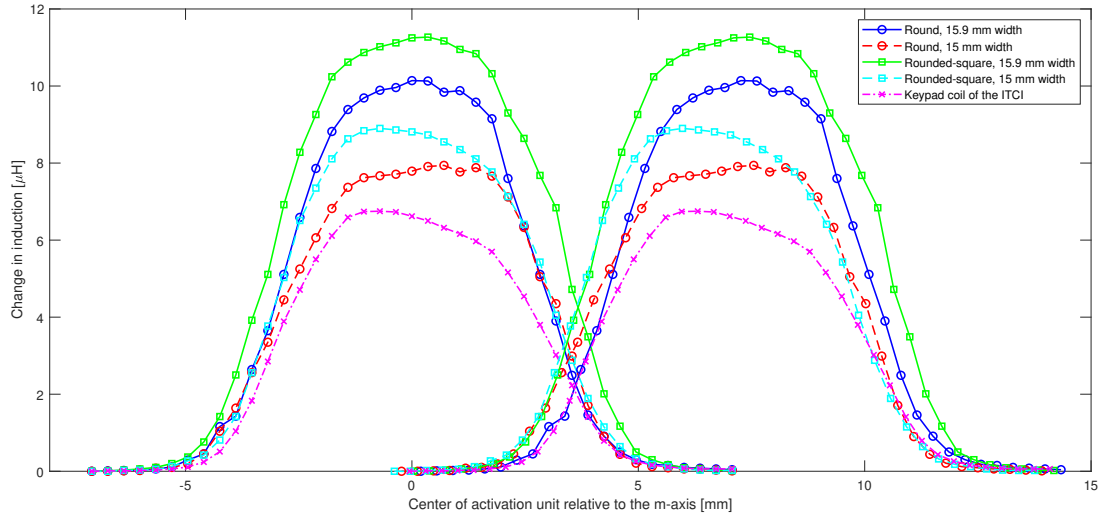

Fig. 8: The change in inductance of PCB coils with respect to the center of the AU with a flat contact surface. The curves in the left show the results for the measured middle coils of the sensor PCBs and the curves in the right show the superimposed results by the distance from C_s to C_m.

higher sensitivity to AU movements. As the activation curves showed, sensor PCBs with 15.9 mm width had a higher inductance change and slightly larger activation range than sensor PCBs with 15 mm width due to the higher number of coil turns. Sensor PCBs with rounded-square coils had slightly higher and larger activation than sensor PCBs with round coils as a result of coil geometry. Moreover, activation of the coils were higher and larger for all types of the developed sensor PCBs than the keypad coils of the ITCI.

The empty area between the coils was smaller for rounded-square coils than round coils due to the coil geometry. Therefore, superimposition of the induction change measurements resulted in closer curves for rounded-square coils. It means that interpolation of sensor signals can be performed with a higher performance with the sensor PCBs with rounded-square coils. Although the centers of the measured coil and the superimposed coil were slightly closer for the 15 mm width sensor PCBs, it did not result in closer curves due to the higher activation ranges of the 15.9 mm width sensor PCBs. The activation curves were closer for all of the developed sensor PCBs than the keypad sensor PCB of the current version of the ITCI as a result of closer positioning of the coils. Therefore, it can be concluded that a higher performance interpolation of sensor signals is possible with

the developed sensor PCBs.

Developed sensor PCBs have three less command signals than the current version of the ITCI, however 15 command signals can be adequate for the control of assistive robotic devices [5]. By reducing the number of sensors and accommodating all sensors in one-piece sensor PCBs, all of the developed sensor PCBs have 22 - 30 % shorter length and therefore smaller size than the sensor PCBs of the ITCI. Although the sensor PCBs with 15 mm width are smaller in size than the 15.9 mm width sensor PCBs, it would be easier to detect activation with 15.9 mm width PCBs.

V. Conclusions and Further Work

In this paper, we developed four different compact one-piece sensor PCBs incorporating inductive sensor coils with different sizes and coil geometries for the design of a noninvasive tongue-robotic interface. We measured the electrical parameters of the developed sensor coils to detect activation by AUs with different contact surfaces and compared them with the coils of keypad area of the ITCI.

The AU with a flat contact surface resulted in higher and wider activation of the coils than the spherical AU. Rounded-square shaped coils had slightly higher and wider activation than round coils. Although the sensor PCBs with 15 mm width are smaller in size, the sensor PCBs with 15.9 mm width had higher activation by an AU. All of the developed sensor PCBs are smaller in size and allow better interpolation of sensor signals than the keypad sensor PCB of the current version of the ITCI.

The next step in developing a high performance noninvasive tongue interface will be the packing and encapsulation of the tongue interface components in a mouthpiece. Further, a frame with an integrated AU will be mounted on the system to develop a noninvasive tongue-robotic interface. Developed interface will be used to control multiple grasps of a soft hand exoskeleton. Moreover, comfort level of the interface perceived by users and effects of learning on task performance will be investigated.

References

[1] C. Lo, Y. Tran, K. Anderson, A. Craig, and J. Middleton, "Functional priorities in persons with spinal cord injury: using discrete choice experiments to determine preferences," *Journal of neurotrauma*, vol. 33, no. 21, pp. 1958–1968, 2016.

[2] A. Craig, K. Hancock, and H. Dickson, "A longitudinal investigation into anxiety and depression in the first 2 years following a spinal cord injury," *Spinal Cord*, vol. 32, no. 10, pp. 675–679, 1994.

[3] C.-S. Chung, H. Wang, and R. A. Cooper, "Functional assessment and performance evaluation for assistive robotic manipulators: Literature review," *The journal of spinal cord medicine*, vol. 36, no. 4, pp. 273–289, 2013.

[4] F. Molteni, G. Gasperini, G. Cannaviello, and E. Guanziroli, "Exoskeleton and end-effector robots for upper and lower limbs rehabilitation: narrative review," *PM&R*, vol. 10, no. 9, pp. S174–S188, 2018.

[5] L. N. A. Struijk, L. L. Egsgaard, R. Lontis, M. Gaihede, and B. Bentsen, "Wireless intraoral tongue control of an assistive robotic arm for individuals with tetraplegia," *Journal of neuroengineering and rehabilitation*, vol. 14, no. 1, pp. 1–8, 2017.

[6] C. Lau and S. O'Leary, "Comparison of computer interface devices for persons with severe physical disabilities," *American Journal of Occupational Therapy*, vol. 47, no. 11, pp. 1022–1030, 1993.

[7] F. Kong, M. N. Sahadat, M. Ghovanloo, and G. D. Durgin, "A standalone intraoral tongue-controlled computer interface for people with tetraplegia," *IEEE transactions on biomedical circuits and systems*, vol. 13, no. 5, pp. 848–857, 2019.

[8] B. Yousefi, X. Huo, and M. Ghovanloo, "Using fitts's law for evaluating tongue drive system as a pointing device for computer access," in *2010 Annual International Conference of the IEEE Engineering in Medicine and Biology*. IEEE, 2010, pp. 4403–4406.

[9] X. Huo, J. Wang, and M. Ghovanloo, "Wireless control of powered wheelchairs with tongue motion using tongue drive assistive technology," in *2008 30th Annual International Conference of the IEEE Engineering in Medicine and Biology Society*. IEEE, 2008, pp. 4199–4202.

[10] S. Ostadabbas, S. N. Housley, N. Sebkhi, K. Richards, D. Wu, Z. Zhang, M. G. Rodriguez, L. Warthen, C. Yarbrough, S. Belagaje *et al.*, "Tongue-controlled robotic rehabilitation: A feasibility study in people with stroke." *Journal of Rehabilitation Research & Development*, vol. 53, no. 6, 2016.

[11] L. NS Andreasen Struijk, E. R. Lontis, M. Gaihede, H. A. Caltenco, M. E. Lund, H. Schioeler, and B. Bentsen, "Development and functional demonstration of a wireless intraoral inductive tongue computer interface for severely disabled persons," *Disability and Rehabilitation: Assistive Technology*, vol. 12, no. 6, pp. 631–640, 2017.

[12] D. Johansen, C. Cipriani, D. B. Popović, and L. N. Struijk, "Control of a robotic hand using a tongue control system—a prosthesis application," *IEEE Transactions on Biomedical Engineering*, vol. 63, no. 7, pp. 1368–1376, 2016.

[13] M. Mohammadi, H. Knoche, M. Thøgersen, S. H. Bengtson, M. A. Gull, B. Bentsen, M. Gaihede, K. E. Severinsen, and L. N. A. Struijk, "Eyes-free tongue gesture and tongue joystick control of a five dof upper-limb exoskeleton for severely disabled individuals," *Frontiers in Neuroscience*, vol. 15, 2021.

[14] S. Muus, "Produkter – TKS A/S," Apr 2021. [Online]. Available: https://tks-technology.dk/produkter/#itongue

[15] E. R. Lontis and L. N. Struijk, "Design of inductive sensors for tongue control system for computers and assistive devices," *Disability and Rehabilitation: Assistive Technology*, vol. 5, no. 4, pp. 266–271, 2010.

[16] H. A. Caltenco, B. Breidegard, B. Jönsson, and L. N. Andreasen Struijk, "Understanding computer users with tetraplegia: Survey of assistive technology users," *International Journal of Human-Computer Interaction*, vol. 28, no. 4, pp. 258–268, 2012.

[17] O. Kirtas, M. Mohammadi, B. Bentsen, P. Veltink, and L. N. A. Struijk, "Design and evaluation of a noninvasive tongue-computer interface for individuals with severe disabilities," in *2021 IEEE 21st International Conference on Bioinformatics and Bioengineering (BIBE)*. IEEE, 2021, pp. 1–6.

[18] M. Mohammadi, H. Knoche, M. Gaihede, B. Bentsen, and L. N. A. Struijk, "A high-resolution tongue-based joystick to enable robot control for individuals with severe disabilities," in *2019 IEEE 16th International Conference on Rehabilitation Robotics (ICORR)*. IEEE, 2019, pp. 1043–1048.